Original Article

The value of predicting neoadjuvant chemotherapy early efficacy in nasopharyngeal carcinoma based on amide proton transfer imaging and diffusion weighted imaging

Yulin Zhang[1,2], Guomin Li[1], Jinyan Chen[1], Meien Jiang[1], Yunyu Gao[3], Kunsong Li[4], Hua Wen[1], Jianhao Yan[1,2]^

[1]Department of Medical Imaging, the Affiliated Guangdong Second Provincial General Hospital of Jinan University, Guangzhou, China; [2]The Second School of Clinical Medicine, Southern Medical University, Guangzhou, China; [3]Central Research Institute, United Imaging Healthcare, Shanghai, China; [4]Department of Oncology, the Affiliated Guangdong Second Provincial General Hospital of Jinan University, Guangzhou, China

Contributions: (I) Conception and design: Y Zhang, G Li, J Yan; (II) Administrative support: J Yan; (III) Provision of study materials or patients: Y Zhang, G Li, J Chen, M Jiang, Y Gao, K Li, H Wen; (IV) Collection and assembly of data: Y Zhang, G Li, Jinyan Chen, M Jiang, Y Gao; (V) Data analysis and interpretation: Y Zhang, G Li, J Chen; (VI) Manuscript writing: All authors; (VII) Final approval of manuscript: All authors.

Correspondence to: Jianhao Yan, PhD. Department of Medical Imaging, the Affiliated Guangdong Second Provincial General Hospital of Jinan University, No. 466 Road Xingang, Guangzhou 510317, China; The Second School of Clinical Medicine, Southern Medical University, Guangzhou, China. Email: yanjianhao@163.com.

Background: Early detection of nasopharyngeal carcinoma (NPC) patients who are not sensitive to neoadjuvant chemotherapy (NAC) can guard against overtreatment. This study aimed to evaluate the effectiveness of amide proton transfer (APT) imaging and diffusion-weighted imaging (DWI) in predicting the early response to NAC in patients with NPC.

Methods: This prospective study enrolled fifty patients with biopsy-confirmed NPC from September 2021 to May 2023. Magnetic resonance imaging (MRI) including APT and DWI, was performed before NAC. After NAC, patients were divided into complete response (CR), partial response (PR), and stable disease (SD) and progressive disease (PD) groups based on the Response Evaluation Criteria in Solid Tumours Version 1.1. The Kruskal-Wallis H test was used for statistical analysis. The differences in APT and apparent diffusion coefficient (ADC) values among the different efficacy groups were compared, the receiver operating characteristic (ROC) curve was drawn for statistically significant parameters, and the area under the curve (AUC) was calculated.

Results: Fifty patients (mean age: 47±14 years; 42 males and 8 females) were included in the final analysis (11 were in the CR group, 30 in the PR group, 9 in the SD group, and 0 in the PD group). The ADC values showed no significant differences among the different treatment response groups. The SD group showed significantly lower APT_{max} (P=0.025), $APT_{skewness}$ (P=0.025) and $APT_{90\%}$ (P=0.001) values than the CR and PR groups. Setting $APT_{90\%}$ =3.10% as the cut-off value, optimal diagnostic performance (AUC: 0.831; sensitivity: 0.778; specificity: 0.878) was obtained in predicting the SD group.

Conclusions: APT imaging can predict the early tumour response to NAC in patients with NPC. APT imaging may be superior to DWI in predicting tumour response.

Keywords: Amide proton transfer (APT); diffusion-weighted imaging (DWI); apparent diffusion coefficient (ADC); neoadjuvant chemoradiotherapy; nasopharyngeal carcinoma (NPC); treatment response

Submitted Jan 29, 2024. Accepted for publication Aug 23, 2024. Published online Sep 26, 2024.
doi: 10.21037/qims-24-188
View this article at: https://dx.doi.org/10.21037/qims-24-188

^ ORCID: 0000-0002-5670-1207.

Introduction

Nasopharyngeal carcinoma (NPC), a common head and neck malignancy, is an epithelial malignancy originating from the nasopharyngeal mucosal lining. In accordance with the International Agency for Research on Cancer, there were approximately 133,354 new cases of NPC worldwide and 80,008 deaths in 2020, with the highest prevalence reported in East and Southeast Asia (1).

Although concurrent chemoradiation (CCRT) is the primary curative treatment for locally advanced NPC, several recent trials have crucially confirmed the benefit of neoadjuvant chemotherapy (NAC) combined with CCRT on survival (2-5). Currently, NAC followed by CCRT is recommended as level 2A evidence for NPC patients with either T1, N1–3, or T2–T4, any N lesions by the National Comprehensive Cancer Network Guidelines (6). However, the curative effect of NAC varies from person to person in clinical practice, and approximately 10% of patients do not respond well to NAC (7). Pre-treatment identification of non-responders would facilitate personalised treatment selection, avoiding additional chemotherapy toxicity, treatment duration, and financial burden. Hence, accurately predicting the response to NAC before treatment is vital for the individualised management and prognosis of patients with NPC.

Magnetic resonance imaging (MRI) advances have improved the ability to diagnose NPC and predict and assess tumour responses to treatment (8,9). Diffusion-weighted imaging (DWI) is a functional imaging technology that can stably detect the Gaussian movement of water molecules in biological tissues and quantitatively analyse the internal microenvironment parameters such as cell density and intracellular space, through the apparent diffusion coefficient (ADC) (10). The ADC has been widely used for diagnosing, following up, and predicting treatment responses in many tumours, as it provides structural information regarding tumour cells (11-13). However, the criteria for predicting early treatment response in patients with NPC with ADC prior to treatment have not been harmonised.

In recent years, amide proton transfer (APT) imaging, a subset of chemical exchange saturation transfer (CEST) imaging, has been demonstrated to indirectly detect mobile cellular proteins and amino acids *in vivo* based on the exchange between amide protons and bulk water protons (14-17). APT imaging, as a novel molecular imaging technology, makes it a reliable approach to reflect tumour cell density and proliferation (18). Most studies have focused on the differential diagnosis and histological characteristics of tumours. Recently, certain studies of assessing the treatment responses have been reported (19-21).

This study aimed to determine the value of DWI combined with APT imaging for evaluating and predicting early efficacy of NAC against NPC and thus providing more accurate information for individualised treatment. We present this article in accordance with the STROBE reporting checklist (available at https://qims.amegroups.com/article/view/10.21037/qims-24-188/rc).

Methods

Patients

The study was conducted in accordance with the Declaration of Helsinki (as revised in 2013). The study was approved by institutional ethics board of Guangdong Second Provincial General Hospital (No. 2023-KY-KZ-144-03) and informed consent was taken from all the patients. Fifty individuals with untreated NPC verified by pathological examination from October 2021 to May 2023 were included for further assessment.

The inclusion criteria for patient enrolment were as follows: (I) patients with undifferentiated non-keratinising NPC confirmed by pathological examination; (II) patients with the primary nasopharyngeal lesions with a maximum diameter >1 cm; (III) patients with APT-weighted imaging and DWI before treatment; and (IV) patients who did not undergo chemoradiotherapy or surgery prior to MRI scans.

Patients were excluded based on the following criteria: (I) incomplete periodic follow-up information; (II) inadequate image quality due to obvious signal loss, motion artifacts, and geometrical distortion; (III) concurrent or previous history of tumour.

Clinical data collection

Age, sex, tumour node metastasis (TNM) stage, histological features, institutional treatment, and other demographic and clinical information were noted. All TNM statuses were determined based on the 8th edition of the International Union Against Cancer and the American Joint Committee on Cancer system.

All patients with NPC received standard treatment. MRI examination was performed before NAC in all patients. The three NAC regimens were as follows: (I) gemcitabine +

cisplatin; (II) paclitaxel + cisplatin ± fluorouracil; (3) docetaxel + cisplatin ± fluorouracil.

During treatment, each patient underwent a routine clinical MRI follow-up. After the patient received 2 cycles of NAC, the target lesions were assessed separately by two radiologists on axial T1-weighted contrast-enhanced images, and any disagreements were settled through consensus discussion. The treatment response of the primary tumour was assessed by calculating the relative change percentage of tumour maximum diameter between pre- and post-treatment as $\Delta D = (D_{pre\text{-}treatment} - D_{post\text{-}treatment})/D_{pre\text{-}treatment}$. The patients were split into four groups based on Response Evaluation Criteria in Solid Tumours Version1.1 (22), complete response (CR, ΔD =100%), partial response (PR, $\Delta D \geq 30\%$), stable disease (SD, $-20\% < \Delta D < 30\%$), and progressive disease (PD, $\Delta D \leq -20\%$).

MRI study

All patients were scanned using a 3T MRI scanner (uMR 780; United Imaging Healthcare, Shanghai, China) with a 24-channel head and neck joint coil. Imaging scans ranged from the base of the skull to the sternoclavicular joint. A routine MRI was performed to determine the sites of the NPC lesions. In addition to T1-weighted imaging (T1WI) in the axial, coronal, and sagittal planes [repetition time (TR)/echo time (TE) = 805 ms/8.08 ms, field of view (FOV) =220 mm × 220 mm; slice thickness =4 mm; slice gaP =20 mm], T2-weighted imaging (T2WI) in the axial plane (TR/TE =4,123 ms/93.92 ms, FOV =220 mm × 220 mm, slice thickness =5 mm; slice gap =20 mm), DWI (TR/TE =2,734 ms/66.3 ms, FOV =250 mm × 250 mm, slice thickness =5 mm, slice gap =20 mm, b values =0 and 600 s/mm^2), and contrast-enhanced T1WI, APT imaging was performed for each patient. ADC maps were produced from both b-values mentioned above. To avoid the influence of contrast agents on APT scanning, APT scanning was performed before enhanced scanning. To eliminate the influence of B0 field inhomogeneity on the APT images, zero-order symmetrical mode (S_0) and water saturation shift referencing (WASSR) techniques were corrected before APT imaging. The maximum cross-sectional area of the solid tumour was selected for single-layer S_0, WASSR, and APT imaging. The greatest cross-section of each solid primary tumour was selected for single-slice APT imaging. The S_0, WASSR, and APT sequences possessed the same plane and spatial resolution and used a two-dimensional (2D) single-shot turbo spin-echo sequence with chemical shift-selective fat suppression. The sequence parameters were as follows: TR/TE =4,500 ms/39.9 ms, 230×230 mm; slice thickness, 6 mm; the recovery time is roughly 2,700 ms. The difference is that the number of S_0 images is 1, WASSR acquires 11 images in the range of –1 to 1 ppm (frequency shift step 0.2 ppm), and APT at –4.5 to 4.5 ppm acquires 31 images. The APT sequence uses 10 Gaussian saturation radio frequency (RF) pulses each having a duration of 100 ms and interleaved by a 10 ms delay. The average CEST power is 2 μT. The scanning time for APT imaging was approximately 3 min 30 s.

APT image processing

APT imaging data were analysed using CEST-MATLAB (Math Works, Natick, Mass) provided by uMR, and magnetisation transfer ratio asymmetry (MTR_{asym}) was performed. The APT signal is represented by MTR_{asym} that was calculated using the following equation:

$$MTR_{asym}(3.5ppm) = \frac{S_{sat}(-3.5ppm) - S_{sat}(+3.5ppm)}{S_0} \quad [1]$$

where $MTR_{asym}(3.5ppm)$ was the magnetization transfer ratio asymmetry at +3.5 ppm offset frequency, and S_{sat} and S_0 are the signal intensity obtained with and without selective saturation pulse, respectively.

Image analysis

First, the tumours were identified on conventional anatomical images namely, T1WI, T2WI, and contrast-enhanced T1WI. The region of interest (ROI) of the primary NPC was manually drawn on the APT and ADC images using the ImageJ software (National Institute of Health, Bethesda, MD, USA), which best represented the overall tumour signal, covering the greatest solid portion of the tumour. Overt haemorrhages, air spaces, necrosis, and cysts were excluded. Histogram analysis was performed on tumour regions to obtain imaging parameters such as the mean, kurtosis, skewness, and percentile value for the 90th percentiles. The analysis of all images and the measurement of APT and ADC values were conducted separately in consensus by two radiologists (G.L. and Y.Z. who possess 10 and 5 years of expertise in head and neck imaging, respectively), and the mean value of the two measurements was used as the measurement result.

Statistical analysis

SPSS 25 (IBM SPSS Statistics Version 20, Chicago, IL,

Table 1 Clinical features of the 50 patients with NPC

Factors	CR	PR	SD
Age (years)			
Median	50	50	47
Range	25–61	20–78	28–73
Gender			
Male	9	26	7
Female	2	4	2
Primary tumour staging			
T1	3	1	0
T2	3	11	1
T3	4	12	7
T4	1	6	1
Nodal staging			
N0	0	0	0
N1	1	5	1
N2	7	20	7
N3	3	5	1
Overall stage			
I	0	0	0
II	1	3	0
III	5	18	3
IV	5	9	6

NPC, nasopharyngeal carcinoma; CR, complete response; PR, partial response; SD, stable disease.

USA) was used for statistical analysis. The intraclass correlation coefficient (ICC) was calculated for APT- and ADC-related parameters to assess inter-observer agreement. Each MRI value was expressed as the median (25th–75th percentile). The Kruskal-Wallis *H* test was used to assess any significant differences between groups with different clinical phases or treatment responses. Statistical significance was set at $P<0.05$. To compute the area under the curve (AUC), cut-off value, sensitivity, and specificity, the receiver operating characteristic (ROC) curve analysis was conducted.

Results

In this study, 50 patients with undifferentiated NPC (mean age: 50 years; range, 20–78 years) were included. In accordance with the treatment efficacy evaluation, 11 patients were assigned to the CR group, 30 to the PR group, 9 to the SD group and none to the PD group. *Table 1* lists the patient characteristics. There were no statistically significant differences in age, sex, or TNM stage among the CR, PR, and SD groups.

ICC for the inter-observer agreements showed excellent agreement for the APT (0.89) and ADC (0.82).

Relationship between the ADC-related parameters and tumour response

Table 2 shows the comparisons of ADC-derived histogram parameters among the three groups. There was no

Table 2 ADC-related parameters for different treatment response groups

ADC value ($\times10^{-3}$ mm^2/s)	Group			P value
	CR (n=11)	PR (n=30)	SD (n=9)	
Mean	0.95 (0.82–1.15)	0.91 (0.85–1.08)	0.92 (0.84–0.97)	0.731
Max	2.03 (1.45–2.14)	2.22 (1.69–2.53)	2.12 (1.77–2.48)	0.402
Min	0.40 (0.31–0.50)	0.33 (0.14–0.47)	0.30 (0.12–0.47)	0.250
Skewness	1.10 (0.15–1.65)	1.08 (0.75–1.58)	1.75 (0.99–2.06)	0.292
Kurtosis	3.47 (0.62–6.81)	2.22 (0.78–5.44)	6.77 (2.16–8.72)	0.204
90%	1.20 (1.04–1.56)	1.30 (1.09–1.57)	1.17 (1.08–1.31)	0.466

The ADC values are expressed as the median (25th–75th percentile). ADC, apparent diffusion coefficient; CR, complete response; PR, partial response; SD, stable disease.

Table 3 APT-related parameters for different treatment response groups

APT value (%)	Group			P value
	CR (n=11)	PR (n=30)	SD (n=9)	
Mean	2.56 (1.60–2.79)	2.18 (1.74–2.59)	1.65 (1.08–2.46)	0.497
Max	8.93 (5.97–9.92)	7.90 (6.92–8.89)	4.72 (3.49–7.05)	0.025*
Min	−1.87 (−4.18 to −0.38)	−1.51 (−2.76 to −0.69)	−1.09 (−3.28 to −0.63)	0.915
Skewness	0.62 (0.28 to 1.22)	0.37 (−0.10 to 1.00)	−0.66 (−1.27 to −0.07)	0.025*
Kurtosis	4.34 (2.76–6.55)	4.44 (2.96–5.71)	4.30 (3.48–5.80)	0.865
90%	4.32 (4.04–5.45)	3.76 (3.45–4.13)	2.66 (1.86–3.05)	0.001**

The APT values are expressed as the median (25th–75th percentile). **, P<0.01 indicates significant difference; *, P<0.05 indicates significant difference. APT, amide proton transfer; CR, complete response; PR, partial response; SD, stable disease.

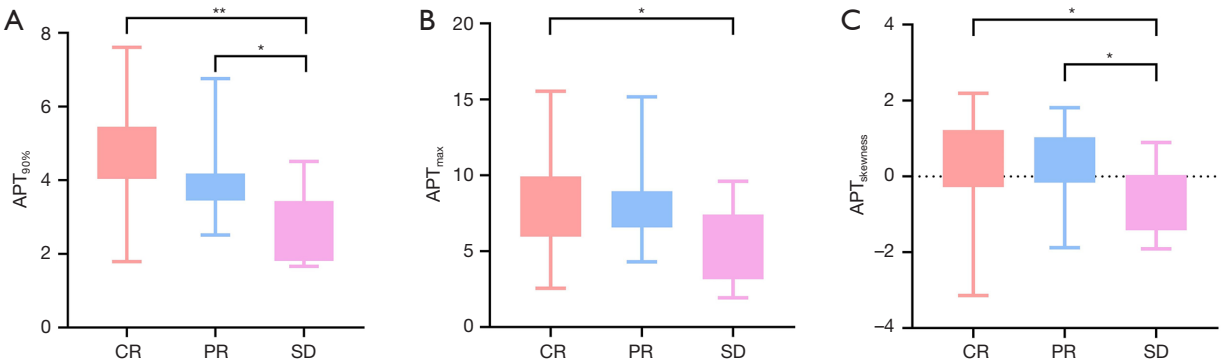

Figure 1 Comparison of APT values, including $APT_{90\%}$, APT_{max} and $APT_{skewness}$ among the CR, PR, and SD groups. **, P<0.01 indicates significant difference; *, P<0.05 indicates significant difference. APT, amide proton transfer; CR, complete response; PR, partial response; SD, stable disease.

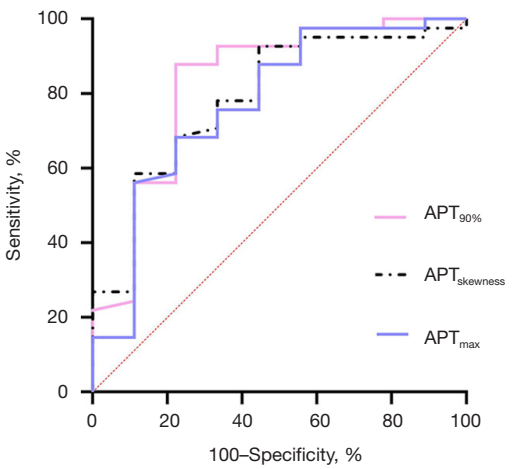

Figure 2 ROC analyses of $APT_{90\%}$, APT_{max} and $APT_{skewness}$ in identifying the patient of the SD group. APT, amide proton transfer; ROC, receiver operating characteristic; SD, stable disease.

significant difference in ADC values among the CR, PR and SD groups (P>0.05).

Relationship between the APT-related parameters and tumour response

Table 3 presents the comparisons of the APT imaging-derived histogram parameters among the treatment response groups. The SD group showed significantly lower $APT_{skewness}$ (P=0.025) and $APT_{90\%}$ (P=0.001) than the CR and PR groups, but no significant differences were observed in APT_{mean} and $APT_{kurtosis}$ (all P>0.05).

Figure 1A-1C show the results of pairwise comparisons of APT signals, including $APT_{90\%}$, APT_{max} and $APT_{skewness}$ between the three groups. We observed a downward trend, particularly in $APT_{90\%}$.

Figure 2 the ROC analysis results revealed that the AUC

of the ROC curve of $APT_{90\%}$ (0.831) was higher than those of APT_{max} (0.774) and $APT_{skewness}$ (0.787). Setting $APT_{90\%}$ =3.10% as the cut-off value, optimal diagnostic performance (AUC: 0.831; sensitivity: 0.778; specificity: 0.878) was obtained in predicting the SD group.

Representative cases are presented in *Figures 3-5*.

Discussion

Accurately predicting the response to NAC may improve the prognosis of NPC by providing alternative treatment for patients who are insensitive to NAC, thus avoiding undesirable chemotherapy-related toxicities. The purpose of the present research was to analyse and compare the value of APT and ADC in predicting the early therapeutic response to NAC in NPC. In this study, we used histogram analysis to provide information regarding intratumoral heterogeneity that adopts a voxel-by-voxel technique to calculate the ADC and APT values for every voxel within the ROI (19,23,24). In this study, $APT_{90\%}$ was the best APT parameter to indicate poor response to NAC in patients with NPC. $APT_{90\%}$ has a significant advantage over APT_{mean}, APT_{max}, APT_{min}, $APT_{skewness}$, and $APT_{kurtosis}$ in that it is more repeatable and statistically less impacted by random fluctuations (25).

While ADC has been demonstrated to be a feasible imaging biomarker for prognostic purposes in many malignancies, our study revealed that there was no significant difference in ADC across the three groups prior to treatment, which is consistent with previous reports by Hong *et al.* (26), Chen *et al.* (27) and Tangyoosuk *et al.* (28). However, prior studies have noted that pre-treatment ADC can predict the prognosis of patients with NPC (11,29-31). Therefore, whether pre-treatment ADC can be used as a predictor of therapeutic response remains controversial and may be related to the influence of various factors such as DWI parameter setting in different centres, ROI selection, sample size, and tumour heterogeneity. This study illustrated the limited value of pre-treatment ADC in predicting the early efficacy of NAC in NPC.

Compared with ADC, APT imaging has good application prospects for predicting the early efficacy of NAC in NPC. First, the APT value is positively correlated with tumour cell density and proliferation (32-34), and is associated with abnormal synthesis and overexpression of intracellular mobile proteins and peptides. Malignant

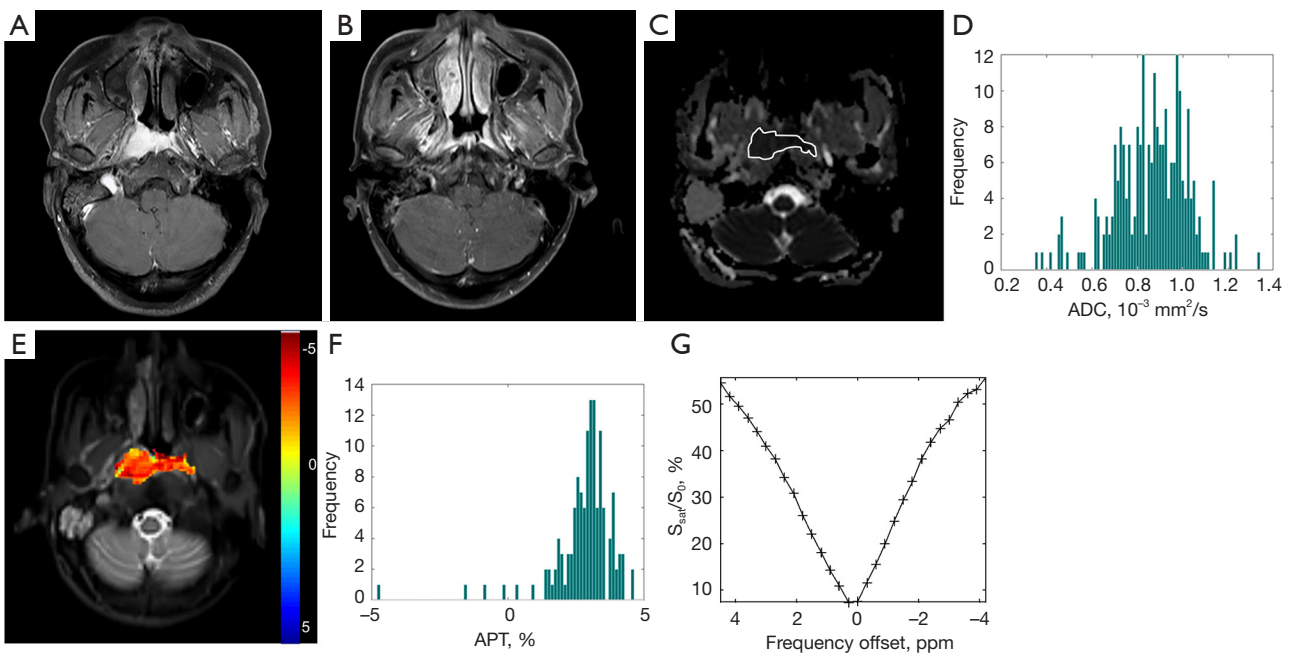

Figure 3 Pictures of a 26-year-old man with NPC in the CR group. (A,B) contrast-enhanced T1WI before and after NAC, after NAC, the mass exhibited a marked decrease in size and was almost indistinguishable. (C-G) ADC map, ADC histogram ($ADC_{90\%}$ =1.04×10^{-3} mm^2/s), APT image, APT histogram ($APT_{90\%}$ =3.84%), and the Z-spectra before treatment, respectively. ADC, apparent diffusion coefficient; APT, amide proton transfer; NPC, nasopharyngeal carcinoma; CR, complete response; T1WI, T1-weighted imaging; NAC, neoadjuvant chemotherapy.

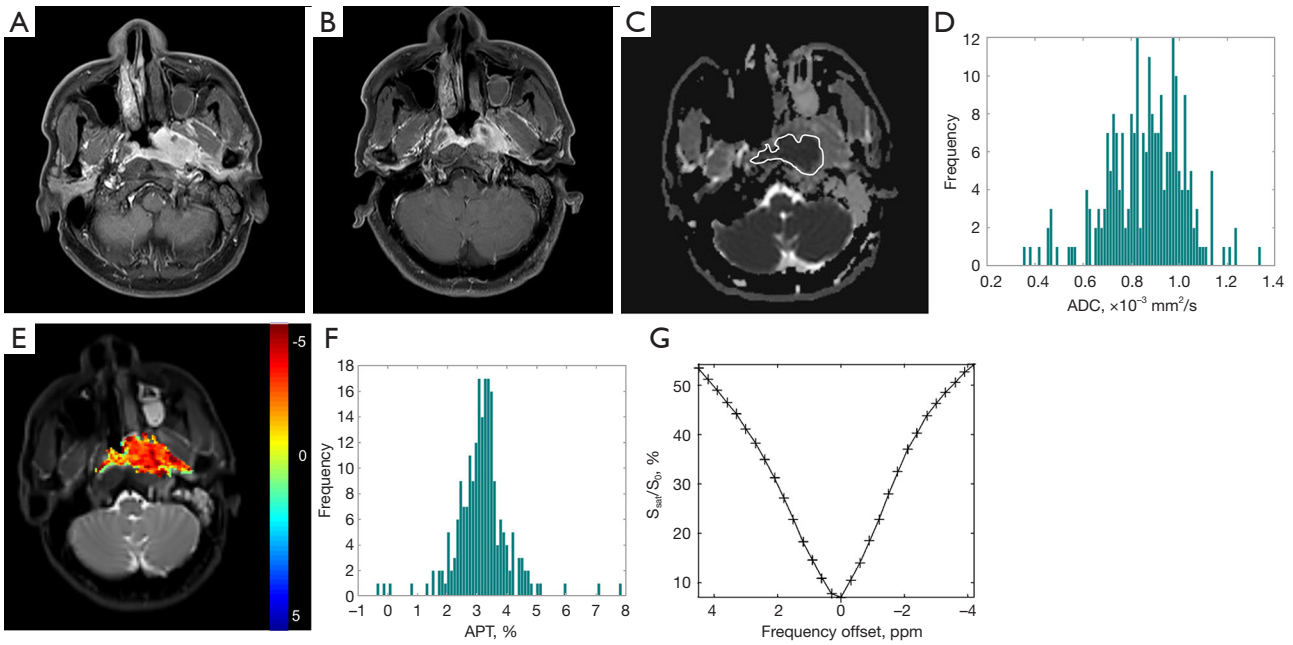

Figure 4 Pictures of a 55-year-old man with NPC in the PR group. (A,B) contrast-enhanced T1WI before and after NAC, after NAC, the mass exhibited a partial decrease in size with a residual tumour remaining at the left posterior pharyngeal wall. (C-G) ADC map, ADC histogram ($ADC_{90\%}$ =0.97×10^{-3} mm^2/s), APT image, APT histogram ($APT_{90\%}$ =4.13%), and the Z-spectra before treatment, respectively. ADC, apparent diffusion coefficient; APT, amide proton transfer; NPC, nasopharyngeal carcinoma; PR, partial response; T1WI, T1-weighted imaging; NAC, neoadjuvant chemotherapy.

tumours are generally associated with more active mitosis, higher cell density, and increased synthesis of free proteins and peptides, ultimately leading to increased APT values. Second, APT is related to the degree of tumour angiogenesis (35). Zheng *et al.* (36) found that a high protein and peptide content in blood increases the APT value. Finally, APT was shown to have a relationship with PH (37), accounting for approximately 34%. However, the contribution of the possible PH variation to the measured APT value may be minimal in the tumors, because the intracellular PH is almost the same as that in the different tumor or different tumor grades (38). APT_{max}, $APT_{skewness}$ and $APT_{90\%}$ was lower in the SD group than the CR and PR groups, which was in accordance with previous findings (39,40). As a result, pre-therapeutic APT values exhibited good prediction performance for the early tumour response in NPC patients after NAC.

Moreover, tumours sensitive to chemotherapy have more tumour cells in the active phase of proliferation, active mitosis, and increased neovascularization, which is conducive to the entry of chemotherapeutic drugs into the tumour to interfere with the division and proliferation of cancer cells. Therefore, patients with high APT values before chemotherapy are often more sensitive to chemotherapy (29). Nishie *et al.* found that the response of rectal cancer to NAC was in inverse proportion to the APT before treatment, whose studies used APT before treatment as the observation indicators (20). The results of these previous research are contrary to ours, and this may be related to the pathological components of the tumour. Certain studies have demonstrated that tumours containing mucin (abundant extracellular/intracellular protein), which are considered to have high APT values, are insensitive to chemotherapy (41).

Typically, the higher the proliferative activity of the tumour, the higher the proportion of tumour cells in the division phase and the more proteins synthesised, which is more conducive to the interference of chemotherapy drugs with tumour cellular proliferation. The APT value can reflect the protein in the tissue at the cellular molecular level, reflect the proliferation activity and cell density of tumour cells by protein content, and predict the sensitivity to chemotherapy. However, ADC can quantitatively analyse the degree of diffusion of water molecules in the

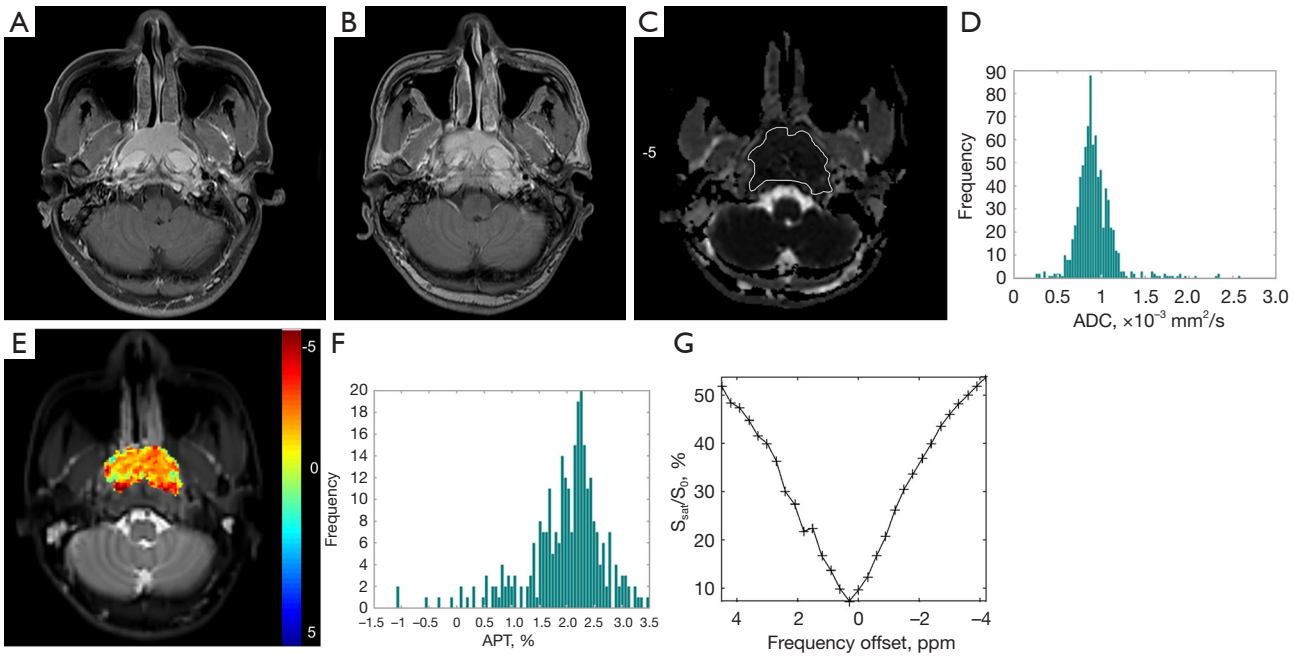

Figure 5 Pictures of a 33-year-old man with NPC in the SD group. (A,B) contrast-enhanced T1WI before and after NAC, after NAC, the mass exhibited almost no decrease in size with residual tumour remaining at the bilateral posterior pharyngeal wall. (C-G) ADC map, and ADC histogram ($ADC_{90\%}$ =1.12×10^{-3} mm^2/s), APT image, APT histogram ($APT_{90\%}$ =2.68%), and the Z-spectra before treatment, respectively. ADC, apparent diffusion coefficient; APT, amide proton transfer; NPC, nasopharyngeal carcinoma; SD, stable disease; T1WI, T1-weighted imaging; NAC, neoadjuvant chemotherapy.

interstitial spaces (between cells), which is directly related to cell density (42), and has certain limitations for the intuitive performance of the proliferation and division of tumour cells. APT values are indicative of both the activity and density of tumour cells, whereas ADC values mainly reflect the density of tumour cells. This could be the reason why APT imaging is a better predictor of the efficacy of early chemotherapy in patients with NPC than ADC imaging.

There are some limitations of our study that must be acknowledged. First, this was a single-centre, small-sample size study with selection bias. Moreover, the distribution of patients in each group was not balanced, and this affected the results of the statistical analysis. More extensive multicentre studies are needed to strengthen these results. Second, just two b-values were employed in the ADC measurements in this study, and therefore, the ADC measurements may be unreliable. Third, we used 2D-APT that only scans a single slice of the tumour. Therefore, it is not possible to comprehensively evaluate NPC. Due to the heterogeneity of the tumour, a single slice does not fully reflect the tumour. In future experiments, three-dimensional (3D)-APT will be used to evaluate tumours comprehensively; however, it requires a long scanning time. Fourth, ADC and APT were not used to comprehensively analyse this study's long-term treatment efficacy. Therefore, further studies are required to confirm the correlation between the ADC and APT values and the long-term prognosis of radiotherapy and chemotherapy. Finally, this study was limited to evaluating chemotherapy efficacy by imaging, which may have caused errors in the efficacy results.

In conclusion, pre-therapeutic APT imaging can be used to predict tumour response to NAC in NPC. APT imaging could be superior to ADC imaging in predicting tumour response.

Acknowledgments

Funding: This study received funding from the clinical Research Program of Guangdong Second Provincial General Hospital (Project No. 3D-A2021006) and Science

and Technology Projects in Guangzhou (Project No. 2023A03J0760).

Footnote

Reporting Checklist: The authors have completed the STROBE reporting checklist. Available at https://qims.amegroups.com/article/view/10.21037/qims-24-188/rc

Conflicts of Interest: All authors have completed the ICMJE uniform disclosure form (available at https://qims.amegroups.com/article/view/10.21037/qims-24-188/coif). Y.G. is from Central Research Institute, United Imaging Healthcare. The other authors have no conflicts of interest to declare.

Ethical Statement: The authors are accountable for all aspects of the work in ensuring that questions related to the accuracy or integrity of any part of the work are appropriately investigated and resolved. The study was conducted in accordance with the Declaration of Helsinki (as revised in 2013). The study was approved by ethics board of Guangdong Second Provincial General Hospital (No. 2023-KY-KZ-144-03) and informed consent was taken from all the patients.

References

1. Sung H, Ferlay J, Siegel RL, Laversanne M, Soerjomataram I, Jemal A, Bray F. Global Cancer Statistics 2020: GLOBOCAN Estimates of Incidence and Mortality Worldwide for 36 Cancers in 185 Countries. CA Cancer J Clin 2021;71:209-49.
2. Zhang Y, Li WF, Liu X, Chen L, Sun R, Sun Y, Liu Q, Ma J. Nomogram to predict the benefit of additional induction chemotherapy to concurrent chemoradiotherapy in locoregionally advanced nasopharyngeal carcinoma: Analysis of a multicenter, phase III randomized trial. Radiother Oncol 2018;129:18-22.
3. Sun Y, Li WF, Chen NY, Zhang N, Hu GQ, Xie FY, et al. Induction chemotherapy plus concurrent chemoradiotherapy versus concurrent chemoradiotherapy alone in locoregionally advanced nasopharyngeal carcinoma: a phase 3, multicentre, randomised controlled trial. Lancet Oncol 2016;17:1509-20.
4. Cavalieri S, Licitra L. Induction chemotherapy is the best timekeeper in nasopharyngeal carcinoma. Cancer 2020;126:3624-6.
5. Peng H, Chen L, Li WF, Guo R, Mao YP, Zhang Y, Guo Y, Sun Y, Ma J. Tumor response to neoadjuvant chemotherapy predicts long-term survival outcomes in patients with locoregionally advanced nasopharyngeal carcinoma: A secondary analysis of a randomized phase 3 clinical trial. Cancer 2017;123:1643-52.
6. Colevas AD, Yom SS, Pfister DG, Spencer S, Adelstein D, Adkins D, et al. NCCN Guidelines Insights: Head and Neck Cancers, Version 1.2018. J Natl Compr Canc Netw 2018;16:479-90.
7. Liu Z, Zou L, Yang Q, Qian L, Li T, Luo H, Che C, Lei Y, Chen P, Qiu C, Liu X, Wu Y, Luo D. Baseline Amide Proton Transfer Imaging at 3T Fails to Predict Early Response to Induction Chemotherapy in Nasopharyngeal Carcinoma. Front Oncol 2022;12:822756.
8. Lu L, Li Y, Li W. The Role of Intravoxel Incoherent Motion MRI in Predicting Early Treatment Response to Chemoradiation for Metastatic Lymph Nodes in Nasopharyngeal Carcinoma. Adv Ther 2016;33:1158-68.
9. Li Y, Li X, Yu X, Lin M, Ouyang H, Xie L, Shang Y. Investigating the value of arterial spin labeling and intravoxel incoherent motion imaging on diagnosing nasopharyngeal carcinoma in T1 stage. Cancer Imaging 2020;20:62.
10. Chung SR, Choi YJ, Suh CH, Lee JH, Baek JH. Diffusion-weighted Magnetic Resonance Imaging for Predicting Response to Chemoradiation Therapy for Head and Neck Squamous Cell Carcinoma: A Systematic Review. Korean J Radiol 2019;20:649-61.
11. Zhao DW, Fan WJ, Meng LL, Luo YR, Wei J, Liu K, Liu G, Li JF, Zang X, Li M, Zhang XX, Ma L. Comparison of the pre-treatment functional MRI metrics' efficacy in predicting Locoregionally advanced nasopharyngeal carcinoma response to induction chemotherapy. Cancer Imaging 2021;21:59.
12. Hirshoren N, Damti S, Weinberger J, Meirovitz A, Sosna J, Eliashar R, Eliahou R. Diffusion weighted magnetic resonance imaging of pre and post treatment

nasopharyngeal carcinoma. Surg Oncol 2019;30:122-5.
13. Huang TX, Lu N, Lian SS, Li H, Yin SH, Geng ZJ, Xie CM. The primary lesion apparent diffusion coefficient is a prognostic factor for locoregionally advanced nasopharyngeal carcinoma: a retrospective study. BMC Cancer 2019;19:470.
14. Zhou J, Zaiss M, Knutsson L, Sun PZ, Ahn SS, Aime S, et al. Review and consensus recommendations on clinical APT-weighted imaging approaches at 3T: Application to brain tumors. Magn Reson Med 2022;88:546-74.
15. Zhou J, Payen JF, Wilson DA, Traystman RJ, van Zijl PC. Using the amide proton signals of intracellular proteins and peptides to detect pH effects in MRI. Nat Med 2003;9:1085-90.
16. Huang J, Chen Z, Park SW, Lai JHC, Chan KWY. Molecular Imaging of Brain Tumors and Drug Delivery Using CEST MRI: Promises and Challenges. Pharmaceutics 2022;14:451.
17. Zhou J, Heo HY, Knutsson L, van Zijl PCM, Jiang S. APT-weighted MRI: Techniques, current neuro applications, and challenging issues. J Magn Reson Imaging 2019;50:347-64.
18. Togao O, Yoshiura T, Keupp J, Hiwatashi A, Yamashita K, Kikuchi K, Suzuki Y, Suzuki SO, Iwaki T, Hata N, Mizoguchi M, Yoshimoto K, Sagiyama K, Takahashi M, Honda H. Amide proton transfer imaging of adult diffuse gliomas: correlation with histopathological grades. Neuro Oncol 2014;16:441-8.
19. Qamar S, King AD, Ai QH, Mo FKF, Chen W, Poon DMC, Tong M, Ma BB, Yeung DK, Wang YX, Yuan J. Pre-treatment amide proton transfer imaging predicts treatment outcome in nasopharyngeal carcinoma. Eur Radiol 2020;30:6339-47.
20. Nishie A, Asayama Y, Ishigami K, Ushijima Y, Takayama Y, Okamoto D, Fujita N, Tsurumaru D, Togao O, Sagiyama K, Manabe T, Oki E, Kubo Y, Hida T, Hirahashi-Fujiwara M, Keupp J, Honda H. Amide proton transfer imaging to predict tumor response to neoadjuvant chemotherapy in locally advanced rectal cancer. J Gastroenterol Hepatol 2019;34:140-6.
21. Chen W, Mao L, Li L, Wei Q, Hu S, Ye Y, Feng J, Liu B, Liu X. Predicting Treatment Response of Neoadjuvant Chemoradiotherapy in Locally Advanced Rectal Cancer Using Amide Proton Transfer MRI Combined With Diffusion-Weighted Imaging. Front Oncol 2021;11:698427.
22. Eisenhauer EA, Therasse P, Bogaerts J, Schwartz LH, Sargent D, Ford R, Dancey J, Arbuck S, Gwyther S, Mooney M, Rubinstein L, Shankar L, Dodd L, Kaplan R, Lacombe D, Verweij J. New response evaluation criteria in solid tumours: revised RECIST guideline (version 1.1). Eur J Cancer 2009;45:228-47.
23. Pham TT, Liney GP, Wong K, Barton MB. Functional MRI for quantitative treatment response prediction in locally advanced rectal cancer. Br J Radiol 2017;90:20151078.
24. Babatürk A, Erden A, Geçim İE. Apparent diffusion coefficient histogram analysis for predicting neoadjuvant chemoradiotherapy response in patients with rectal cancer. Diagn Interv Radiol 2022;28:403-9.
25. Chung WJ, Kim HS, Kim N, Choi CG, Kim SJ. Recurrent glioblastoma: optimum area under the curve method derived from dynamic contrast-enhanced T1-weighted perfusion MR imaging. Radiology 2013;269:561-8.
26. Hong J, Yao Y, Zhang Y, Tang T, Zhang H, Bao D, Chen Y, Pan J. Value of magnetic resonance diffusion-weighted imaging for the prediction of radiosensitivity in nasopharyngeal carcinoma. Otolaryngol Head Neck Surg 2013;149:707-13.
27. Chen Y, Liu X, Zheng D, Xu L, Hong L, Xu Y, Pan J. Diffusion-weighted magnetic resonance imaging for early response assessment of chemoradiotherapy in patients with nasopharyngeal carcinoma. Magn Reson Imaging 2014;32:630-7.
28. Tangyoosuk T, Lertbutsayanukul C, Jittapiromsak N. Utility of diffusion-weighted magnetic resonance imaging in predicting the treatment response of nasopharyngeal carcinoma. Neuroradiol J 2022;35:477-85.
29. Zhang GY, Wang YJ, Liu JP, Zhou XH, Xu ZF, Chen XP, Xu T, Wei WH, Zhang Y, Huang Y. Pretreatment Diffusion-Weighted MRI Can Predict the Response to Neoadjuvant Chemotherapy in Patients with Nasopharyngeal Carcinoma. Biomed Res Int 2015;2015:307943.
30. Xiao-ping Y, Jing H, Fei-ping L, Yin H, Qiang L, Lanlan W, Wei W. Intravoxel incoherent motion MRI for predicting early response to induction chemotherapy and chemoradiotherapy in patients with nasopharyngeal carcinoma. J Magn Reson Imaging 2016;43:1179-90.
31. Qin Y, Yu X, Hou J, Hu Y, Li F, Wen L, Lu Q, Fu Y, Liu S. Predicting chemoradiotherapy response of nasopharyngeal carcinoma using texture features based on intravoxel incoherent motion diffusion-weighted imaging. Medicine (Baltimore) 2018;97:e11676.
32. Song Q, Chen P, Chen X, Sun C, Wang J, Tan B, Liu H,

Cheng Y. Dynamic Change of Amide Proton Transfer Imaging in Irradiated Nasopharyngeal Carcinoma and Related Histopathological Mechanism. Mol Imaging Biol 2021;23:846-53.
33. Sagiyama K, Mashimo T, Togao O, Vemireddy V, Hatanpaa KJ, Maher EA, Mickey BE, Pan E, Sherry AD, Bachoo RM, Takahashi M. In vivo chemical exchange saturation transfer imaging allows early detection of a therapeutic response in glioblastoma. Proc Natl Acad Sci U S A 2014;111:4542-7.
34. Cairns RA, Harris IS, Mak TW. Regulation of cancer cell metabolism. Nat Rev Cancer 2011;11:85-95.
35. Deng X, Liu M, Zhou Q, Zhao X, Li M, Zhang J, Shen H, Lan X, Zhang X, Zhang J. Predicting treatment response to concurrent chemoradiotherapy in squamous cell carcinoma of the cervix using amide proton transfer imaging and intravoxel incoherent motion imaging. Diagn Interv Imaging 2022;103:618-24.
36. Zheng S, van der Bom IM, Zu Z, Lin G, Zhao Y, Gounis MJ. Chemical exchange saturation transfer effect in blood. Magn Reson Med 2014;71:1082-92.
37. Ray KJ, Simard MA, Larkin JR, Coates J, Kinchesh P, Smart SC, Higgins GS, Chappell MA, Sibson NR. Tumor pH and Protein Concentration Contribute to the Signal of Amide Proton Transfer Magnetic Resonance Imaging. Cancer Res 2019;79:1343-52.
38. Qin X, Mu R, Zheng W, Li X, Liu F, Zhuang Z, Yang P, Zhu X. Comparison and combination of amide proton transfer magnetic resonance imaging and the apparent diffusion coefficient in differentiating the grades of prostate cancer. Quant Imaging Med Surg 2023;13:812-24.
39. Liu W, Wang X, Xie S, Liu WV, Masokano IB, Bai Y, Chen J, Zhong L, Luo Y, Zhou G, Li W, Pei Y. Amide proton transfer (APT) and magnetization transfer (MT) in predicting short-term therapeutic outcome in nasopharyngeal carcinoma after chemoradiotherapy: a feasibility study of three-dimensional chemical exchange saturation transfer (CEST) MRI. Cancer Imaging 2023;23:80.
40. Qamar S, King AD, Ai QY, Law BKH, Chan JSM, Poon DMC, Tong M, Mo FKF, Chen W, Bhatia KS, Ahuja AT, Ma BBY, Yeung DK, Wang YX, Yuan J. Amide proton transfer MRI detects early changes in nasopharyngeal carcinoma: providing a potential imaging marker for treatment response. Eur Arch Otorhinolaryngol 2019;276:505-12.
41. Cantero-Recasens G, Alonso-Marañón J, Lobo-Jarne T, Garrido M, Iglesias M, Espinosa L, Malhotra V. Reversing chemorefraction in colorectal cancer cells by controlling mucin secretion. Elife 2022;11:e73926.
42. Guadilla I, Calle D, López-Larrubia P. Diffusion-Weighted Magnetic Resonance Imaging. Methods Mol Biol 2018;1718:89-101.

Cite this article as: Zhang Y, Li G, Chen J, Jiang M, Gao Y, Li K, Wen H, Yan J. The value of predicting neoadjuvant chemotherapy early efficacy in nasopharyngeal carcinoma based on amide proton transfer imaging and diffusion weighted imaging. Quant Imaging Med Surg 2024;14(10):7330-7340. doi: 10.21037/qims-24-188

